

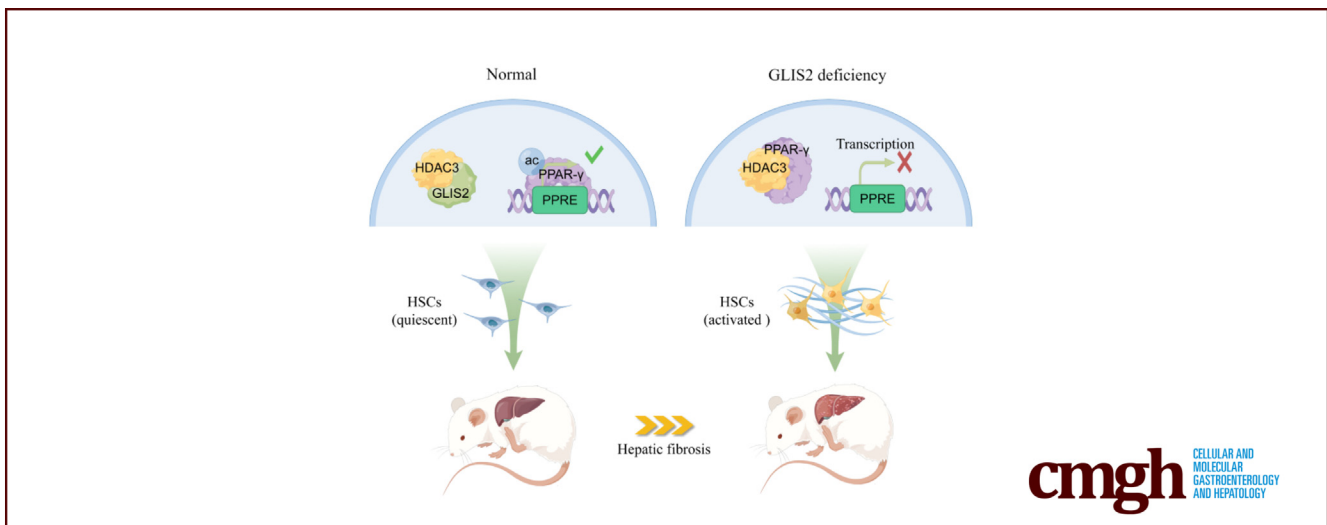
ORIGINAL RESEARCH

GLIS2 Prevents Hepatic Fibrosis by Competitively Binding HDAC3 to Inhibit Hepatic Stellate Cell Activation



Haoye Zhang,¹ Pengcheng Zhou,^{1,2} Wu Xing,³ Limin Chen,¹ Yangmei Zhou,¹ Hui Yang,¹ Kangkang Fu,¹ and Zhenguo Liu^{1,2}

¹Department of Infectious Disease, The Third Xiangya Hospital, Central South University, Changsha, People's Republic of China; ²Hunan Key Laboratory of Viral Hepatitis, Xiangya Hospital, Central South University, Changsha, People's Republic of China; and ³Department of Radiology, Xiangya Hospital, Central South University, Changsha, People's Republic of China



SUMMARY

This study demonstrates the significance of GLIS2 in preserving the normal physiological state of liver tissue. GLIS2 deficiency leads to the development of liver fibrosis in mice, which is caused by activation of the histone deacetylase 3-mediated PPAR- γ signaling pathway in hepatic stellate cells.

BACKGROUND: The role of GLIS2 in fibrotic diseases is controversial. GLIS2 deficiency has been reported to contribute to renal fibrosis in mice and has also been reported to prevent high lipid-induced mice hepatic fibrosis.

METHODS: Hepatic fibrosis in mice was induced by CCl₄. Hematoxylin and eosin, Masson, Sirius red, and enzyme-linked immunosorbent assay were used to detect and evaluate the stage of hepatic fibrosis in humans or mice. A study model of tetracycline-responsive GLIS2 knockout hepatic stellate cells (HSCs) was constructed and named GLIS2-SG-Dox. By adding transforming growth factor β 1 to stimulate the transdifferentiation of HSCs, the activation status of HSCs was comprehensively evaluated from the aspects of cell proliferation, migration, and the amount of lipid droplets. In mechanistic studies, dual-luciferase, coimmunoprecipitation, yeast two-

hybrid system, chromatin immunoprecipitation, and DNA pull-down were performed to investigate or to prove the molecular mechanism that GLIS2 was involved in regulating liver fibrosis. Throughout the study, real-time fluorescence polymerase chain reaction (quantitative reverse-transcription polymerase chain reaction) was used to detect the relative abundance of messenger RNA expression of each target gene, Western blot was used to detect the relative abundance of protein, and immunohistochemistry or immunofluorescence was used to observe the subcellular localization of the target protein.

RESULTS: The expression of GLIS2 was significantly decreased in human liver fibrosis tissues and CCL₄-induced mouse liver fibrosis tissues, especially in HSCs. In the GLIS2-SG-Dox cells, the peroxisome proliferator-activated receptor γ (PPAR- γ) pathway was inactive and cells underwent myofibroblastic transdifferentiation transformation. Overexpression of GLIS2 can increase the acetylation level of PPAR- γ and alleviate CCL₄-induced liver fibrosis in mice. Mechanically, relatively abundant GLIS2 and histone deacetylase 3 (HDAC3) form chelates to avoid the deacetylation of PPAR- γ , so as to maintain the activation level of PPAR- γ signaling pathway in HSCs cells. In this process, HDAC3 acts as a medium for GLIS2 to influence PPAR- γ signaling. Nonetheless, when GLIS2 is absent, HDAC3 deacetylates PPAR- γ , activates HSCs, and leads to liver fibrosis.

CONCLUSIONS: GLIS2 deficiency promotes myofibroblastic transdifferentiation and activation of HSCs. Mechanically, GLIS2 regulates the acetylation of PPAR- γ by competitively binding to HDAC3 in HSCs. (*Cell Mol Gastroenterol Hepatol* 2023;15:355–372; <https://doi.org/10.1016/j.jcmgh.2022.10.015>)

Keywords: GLIS2; Hepatic Fibrosis; PPAR- γ ; HDAC3; Acetylation.

Hepatic stellate cells (HSCs), undifferentiated myofibroblasts derived from the mesoderm, are capable of developing into endothelial cells and hepatic lineages.^{1,2} HSCs have remarkable plasticity (eg they can switch from a quiescent to an activated and back to an inactivated phenotype), making them an appealing target for antifibrotic therapy. The activation of quiescent HSCs (qHSCs) into myofibroblasts (activated HSCs [aHSCs]) has been linked to the development of hepatic fibrosis.^{3–7} During the resting phase, HSCs store retinol and produce a glial fibrillary acidic protein (GFAP). However, when activated and developed into myofibroblast-like cells, the synthesis of extracellular matrix protein and α -smooth muscle actin (α -SMA) was increased while GFAP was gradually lost.⁴

GLIS2, a zinc finger protein, belongs to the Gli-similar family, which also includes the transcription factors GLIS1, GLIS2, and GLIS3.^{8,9} Glis proteins have been linked to several diseases, including cystic kidney disease, diabetes, hypothyroidism, fibrosis, osteoporosis, psoriasis, and cancer.¹⁰ GLIS2 was the most commonly reported gene in fibrosis. For example, it plays an important role in maintaining normal kidney structure and function by preventing apoptosis and fibrosis, and GLIS2 mutation is linked to tubule atrophy and progressive fibrosis.⁹ Furthermore, many genes involved in immune response, inflammation, and fibrosis were upregulated in the kidneys of transgenic mice with GLIS2 mutations.¹¹ There have been few reports on the effect of GLIS2 on hepatic fibrosis.

One of the most adipogenic transcriptional factors, peroxisome proliferator-activated receptor γ (PPAR- γ), is thought to be a biomarker of qHSCs that is lost upon activation.^{12,13} The loss of PPAR- γ is thought to be the primary cause of HSC activation with myofibroblastic transdifferentiation (MTD).¹⁴ MTD could be reversed by restoring PPAR- γ expression in HSCs, demonstrating that a PPAR- γ mediated adipogenic transcriptional program keeps HSCs quiescent.^{12,15} The activation of the PPAR- γ signaling pathway is well accepted to be associated with its acetylation level,¹⁶ which was decreased in hepatic fibrosis.^{17,18} To keep HSCs silent by activating the PPAR- γ pathway, it is necessary to understand the molecular mechanism of PPAR- γ deacetylation in hepatic fibrosis.

In this study, we discovered that GLIS2 inhibited PPAR- γ deacetylation by competitively binding to histone deacetylase 3 (HDAC3), resulting in increased PPAR- γ acetylation in HSCs. Following that, active PPAR- γ enters the nucleus and promotes the transcriptional levels of adipogenic genes, keeping HSCs in a dormant state. It is notable that this GLIS2-dependent mechanism fails to hold in GLIS2-deficient

cells, and in that case HDAC3 deacetylates PPAR- γ and promotes HSC MTD, resulting in the occurrence or progression of hepatic fibrosis. Conclusively, the current study demonstrates that GLIS2 is required for PPAR- γ signaling to maintain HSCs in a quiescent state.

Results


GLIS2 Is Downregulated in Fibrosis Liver Tissues

Pathological examination was conducted on liver biopsy samples collected from patients with fibrosis suspected of having liver cancer, and the results showed that collagen was increased while GLIS2 was significantly decreased in liver tissues with fibrosis aggravation (Figure 1A and B). CCL4 induction was then used to create hepatic fibrosis mice models. Histological staining (hematoxylin and eosin [H&E], Masson, and Sirius red) of livers revealed significant pathological changes and increased collagen fiber accumulation in the model mice (Figure 1C), and serum alanine aminotransferase [ALT], aspartate aminotransferase (AST), and total bilirubin levels were significantly elevated (Figure 1D). Meanwhile, fibrosis-related indicators such as α -SMA; collagen type I, alpha-1 chain (Col1 α 1); and metalloproteinase inhibitor 1 (TIMP1) were significantly increased (Figure 1E and F), indicating that the hepatic fibrosis model was successfully established in mice. GLIS2 was found to be significantly reduced in the livers of fibrosis mice at both the messenger RNA (mRNA) and protein levels (Figure 1E and G). Then, hepatocytes and HSCs were isolated from the livers of the model group and control groups (Figure 1H), and it was discovered that GLIS2 decreased significantly, particularly in HSCs (Figure 1I and J). As a result, HSCs were used to investigate the effect of GLIS2 on hepatic fibrosis.

Generate GLIS2 Deficiency HSCs With CRISPR/Cas9

The immortalized mouse hepatic stellate cell line JS-1¹⁹ was chosen to create a CRISPR/Cas9-based GLIS2 knockout cell model (Figure 2A). Three single guide RNAs (sgRNAs) suitable for spCas9 (NGG) were designed, with sgRNA-2 demonstrating the highest knockout efficiency in the T7E1 assay (Figure 2B). Following transfection and puromycin resistance selection, single cell-derived D3 was chosen for

Abbreviations used in this paper: α -SMA, α -smooth muscle actin; AAV, adeno-associated virus; aHSC, activated hepatic stellate cell; ALT, alanine aminotransferase; AST, aspartate aminotransferase; co-IP, coimmunoprecipitation; Col1 α 1, collagen type I, alpha-1 chain; GFAP, glial fibrillary acidic protein; H&E, hematoxylin and eosin; HDAC3, histone deacetylase 3; HSC, hepatic stellate cell; mRNA, messenger RNA; MTD, myofibroblastic transdifferentiation; PPAR- γ , peroxisome proliferator-activated receptor γ ; PPRE, PPAR response element; qHSC, quiescent hepatic stellate cell; qRT-PCR, quantitative reverse-transcription polymerase chain reaction; sgRNA, single guide RNA; TGF- β 1, transforming growth factor β 1; TIMP1, metalloproteinase inhibitor 1.

 Most current article

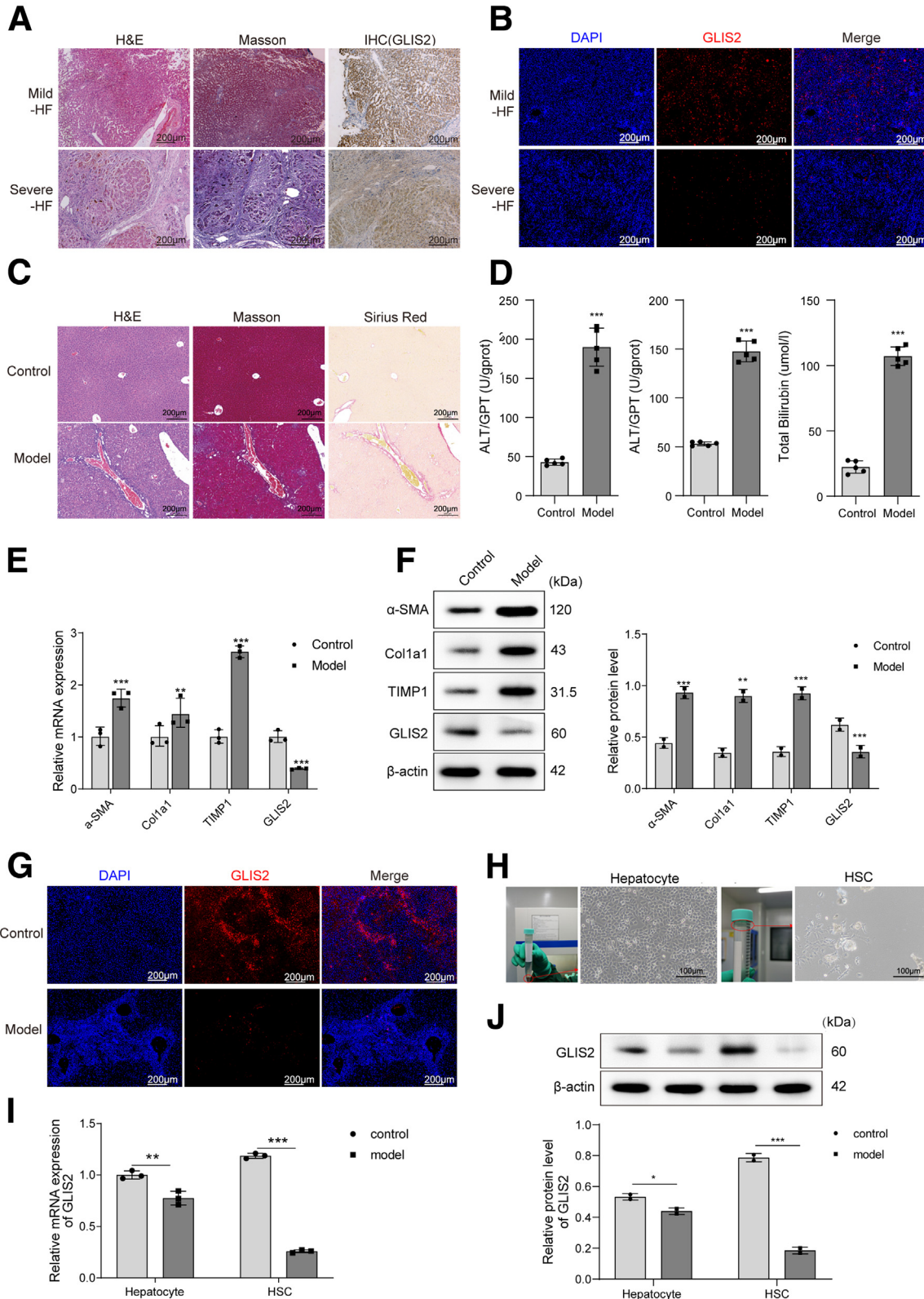
© 2022 The Authors. Published by Elsevier Inc. on behalf of the AGA Institute. This is an open access article under the CC BY-NC-ND license (<http://creativecommons.org/licenses/by-nc-nd/4.0/>).

2352-345X

<https://doi.org/10.1016/j.jcmgh.2022.10.015>

further testing (Figure 2C–E). When doxycycline was added to this system, Cas9 was expressed and knocked GLIS2 down in JS-1 cells. When doxycycline was removed, Cas9 was

terminated, and GLIS2 expression improved (Figure 2F–H), indicating that the GLIS2 knockout cell line based on the Tet-On system was successfully constructed and named GLIS2-SG.



GLIS2 Deficiency Promotes MTD and Activation of HSCs by Inactivating the PPAR- γ Pathway

The GLIS2-SG exhibited aHSC characteristics, as evidenced by increased expression of the aHSC marker P75 neurotrophic receptor (P75NTR) and the decreased expression of the qHSC marker GFAP (Figure 3A and B). Furthermore, GLIS2-SG cells outperformed the control cells in terms of proliferation and migration (Figure 3C and D). Because HSCs are the primary storage site for fat droplets in the liver,^{12,13} the expression levels of adipose-related genes such as PLIN2 (perilipin-2) and ADIPOR1 (adiponectin receptor protein 1), as well as the content of lipid droplets, were checked one after the other to assess the functional changes in HSCs with or without GLIS2,^{18,20,21} and the results showed that they all decreased significantly in GLIS2-SG (Figure 3E-G). Furthermore, it could be seen that all of the results in GLIS2-SG cells were similar to those of transforming growth factor β 1 (TGF- β 1)-induced aHSCs, implying that GLIS2 deficiency in HSCs leads to transdifferentiation and activation of HSCs. However, the TGF- β 1 receptor was significantly elevated in TGF- β 1-induced cells but not in GLIS2-SG (Figure 3A and B), implying that GLIS2 deficiency may be independent of the TGF- β 1 receptor pathway in inducing HSC activation.

Previous research has shown that the inactivation of the PPAR- γ pathway is the primary cause of MTD in stellate cells.¹⁴ The PPAR- γ signaling pathway was then investigated to estimate GLIS2's effect on MTD. When GLIS2 was knocked out by adding doxycycline to JS-1 cells, there was a significant decrease in PPAR- γ targeted genes such as FABP4 (fatty acid binding protein 4), CD36 molecule, and SCD1 (steroyl-Coenzyme A desaturase 1) (Figure 3H and I).^{18,20-22} However, it is also worth noting that PPAR- γ expression at both the mRNA and protein levels in GLIS2-SG cells was not significantly altered (Figure 3H and I). As a transcription factor, GLIS2 did not affect PPAR- γ transcription (Figure 3J). However, the enrichment of PPAR- γ in target gene promoters (FABP4, CD36, and SCD1) was significantly reduced (Figure 3K). These findings suggest that, while GLIS2 deletion reduces the PPAR- γ signaling pathway transcriptional activity and lipid storage capacity, it does not directly regulate PPAR- γ expression.

HDAC3 Acts as an Intermediary for GLIS2 to Affect PPAR- γ

PPAR- γ has been shown to activate downstream target genes through the formation of co-activation complexes

with other proteins such as PGC-1 α .²² The dual-luciferase assay first ruled out the presence of PPAR- γ as a transcription factor on GLIS2 transcription (Figure 4A). Following that, the possibility of a coactivation complex formed by GLIS2 and PPAR- γ was ruled out using the GST pulldown assay, coimmunoprecipitation (co-IP) assay, and yeast two-hybrid system (Figure 4B-D), implying that GLIS2 does not activate its signal transduction pathway by directly acting on PPAR- γ and that some other mechanism is at work.

We searched the proteins interacting with GLIS2 and PPAR- γ (www.hitpredict.org)²³ to find the link between GLIS2 and PPAR- γ signaling, and it turns out that HDAC3 is the only intersection (Table 1). Fortunately, co-IP and yeast two-hybrid system tests confirmed the direct interaction of GLIS2 and HDAC3, as well as HDAC3 and PPAR- γ . Furthermore, when HDAC3 was used as a bait protein, both GLIS2 and PPAR- γ were pulled down in HSCs (Figure 4E-G), indicating that HDAC3 could be an intermediate link in GLIS2-mediated PPAR- γ activation of HSCs.

GLIS2 Regulates the Acetylation of PPAR- γ by Competitively Binding to HDAC3

HDAC3 is a deacetylase that is commonly identified.²⁴⁻²⁶ There was more HDAC3 binding with PPAR- γ in GLIS2-SG cells, leading to a decrease in acetylation (Figure 5A and B). Because inactive PPAR- γ remains in the cytoplasm, rather than entering the nucleus to facilitate transcription of target genes (Figure 5C and D), less PPAR- γ binding to the PPAR response element (PPRE) of downstream target genes such as CD36 was observed (Figure 5E). These findings suggest that HDAC3 inhibits PPAR- γ signaling in GLIS2-SG cells.

Next, HDAC3 was then knocked out using sgRNA in GLIS2-SG cells to see if GLIS2 plays a role in regulating PPAR- γ signaling via HDAC3 (Figure 6A-D). When HDAC3 was removed from the equation, the acetylation level of PPAR- γ increased significantly (Figure 6E and F). Furthermore, GLIS2-SG cell proliferation, migration, and expression of the aHSCs biomarker (P75NTR) were reduced whereas lipid storage and GFAP expression were increased in comparison to the HDAC3 un-knockout group (Figure 6G-K). This demonstrates that reducing HDAC3 can partially reverse the PPAR- γ signal inactivation caused by GLIS2 deficiency.

We then looked into whether GLIS2 influences PPAR- γ acetylation levels to determine HSC status. When the PPAR- γ acetylation activator pioglitazone was added to GLIS2-SG

Figure 1. (See previous page). GLIS2 is downregulated in fibrosis liver tissue. (A) H&E, Masson, and immunohistochemistry (IHC) were used to examine histological changes and the immunoreactivity of GLIS2 in liver samples from patients with varying degrees of hepatic fibrosis (HF). (B) GLIS2 (red) was found in liver samples from patients with varying degrees of HF using immunofluorescence. DAPI was used to visualize the nucleus. (C) H&E, Masson, and Sirius red staining were used to examine histological changes in liver tissues in model and control mice. (D) Enzyme-linked immunosorbent assay was used to detect serum levels of total bilirubin, ALT, and AST in model and control mice ($n = 5$, SD; * $P < .05$; ** $P < .01$; *** $P < .001$). (E, F) The mRNA and protein expression levels of fibrosis-related indices (α -SMA, Col1 α 1, TIMP1) and GLIS2 were determined in model and control mice using qRT-PCR and Western blot ($n = 3$, SD; * $P < .05$; ** $P < .01$; *** $P < .001$). (G) Immunofluorescence detected GLIS2 (red) in mouse liver tissues. DAPI was used to visualize the nucleus. (H) Mice were used to isolate primary mouse hepatocytes (left) and primary HSCs (right). (I, J) qRT-PCR and Western blot were used to detect GLIS2 mRNA and protein expression levels in mouse primary HSCs and liver tissues ($n = 5$, SD; * $P < .05$; ** $P < .01$; *** $P < .001$). GPT, glutamic-pyruvic transaminase.

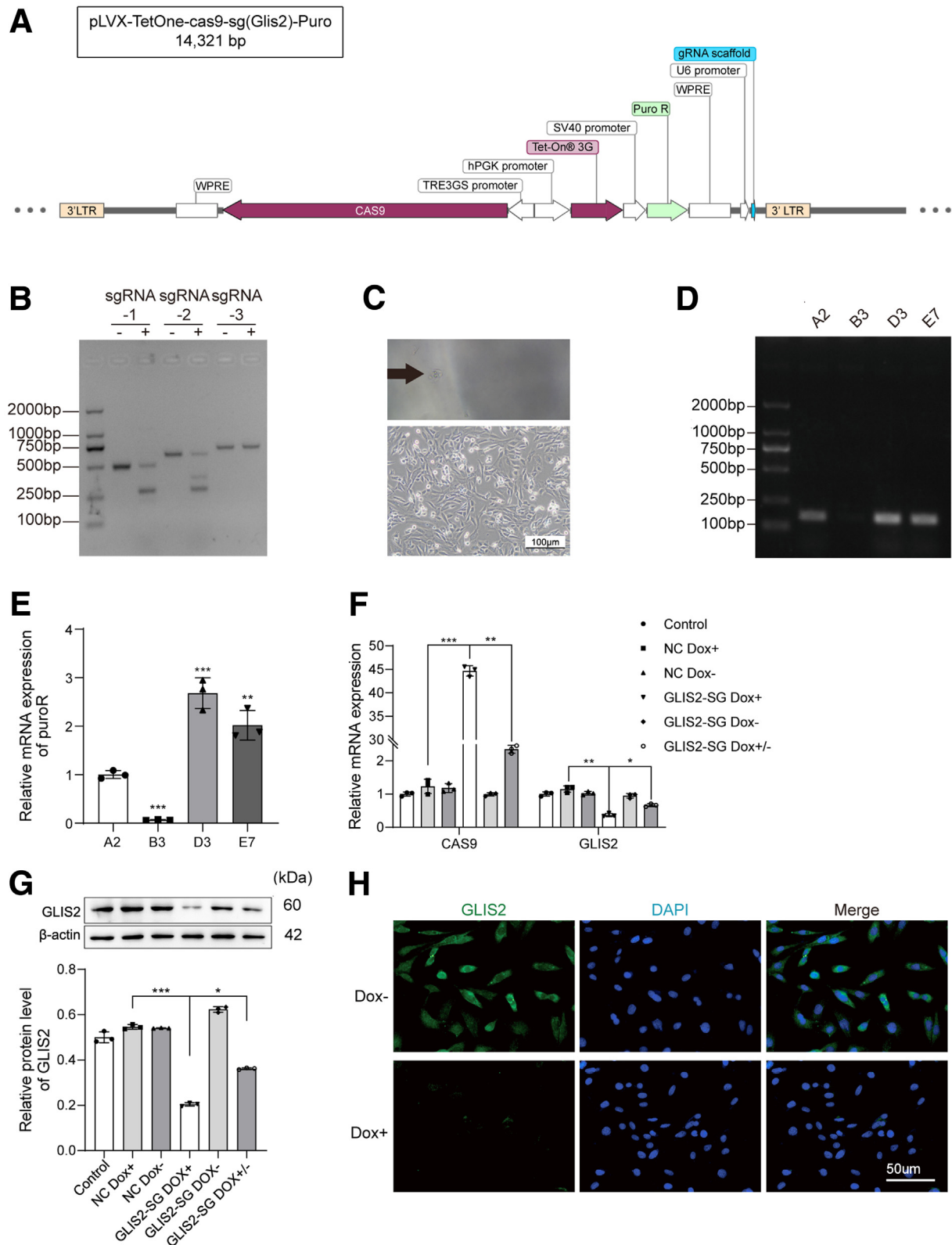


Figure 2. Constructed GLIS2 knockout cell line in HSC lines. (A) Lentiviral knockout vector mapping for mouse GLIS2. Gene knockout in the vector is based on CRISPR/Cas9, and Cas9 expression is controlled by the Tet-On system. (B) The T7E1 assay was used to detect the effect of 3 sgRNAs targeting the mouse GLIS2, with sgRNA-2 having the best knockout effect. (C) GLIS2 deficiency cell lines were created by multiplying single cells. (D, E) Genomic PCR and qRT-PCR were used to detect viral elements integrated into the genomes of different cell lines ($n = 3$, SD; * $P < .05$; ** $P < .01$; *** $P < .001$). (F, G) GLIS2 knockout was confirmed using qRT-PCR and Western blot. Dox+ denotes the addition of doxycycline in cell culture, Dox- denotes the absence of doxycycline, and Dox+/- denotes the addition of doxycycline for culture followed by the removal of doxycycline for continuous culture. ($n = 3$, SD; * $P < .05$; ** $P < .01$; *** $P < .001$). (H) GLIS2 immunofluorescence staining in a GLIS2-SG cell. GLIS2 is green; DAPI is blue. NC, negative control

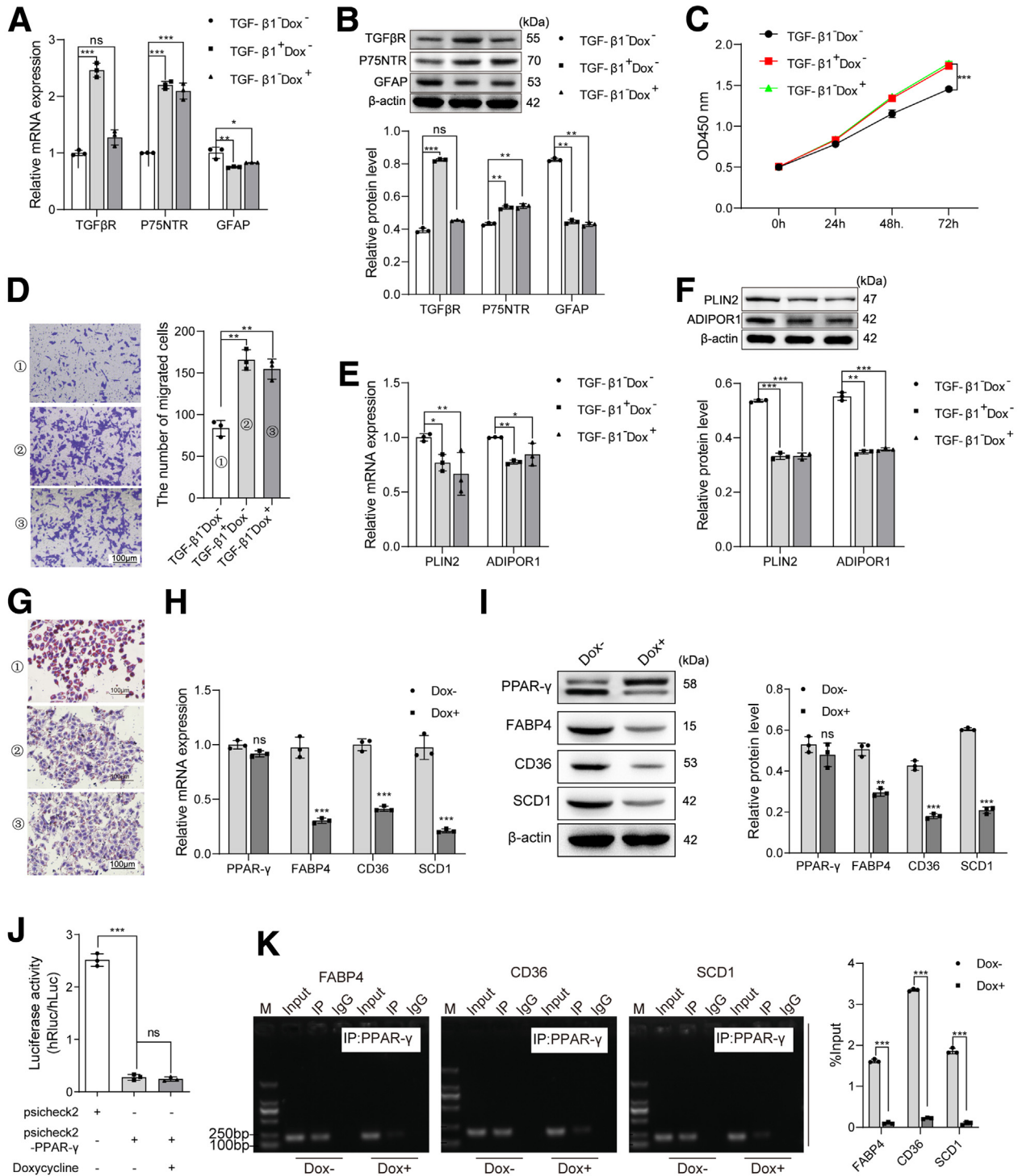


Figure 3. GLIS2 deficiency induces activation and MTD of HSCs by inactivating the PPAR- γ -mediated lipid storage pathway. (A, B) qRT-PCR and Western blot detection of stellate cell status-related genes (P75NTR, GFAP) and TGF- β 1 receptor (TGF β R) mRNA and protein expression levels ($n = 3$, SD; * $P < .05$; ** $P < .01$; *** $P < .001$). (C) The CCK-8 assay was used to monitor cell proliferation induced by GLIS2 knockout or TGF- β 1 induction ($n = 3$, SD; * $P < .05$; ** $P < .01$; *** $P < .001$). (D) Transwell migration assay was used to detect cell migration induced by GLIS2 knockout or TGF- β 1 induction ($n = 3$, SD; * $P < .05$; ** $P < .01$; *** $P < .001$). (E, F) qRT-PCR and Western blot were used to detect the mRNA and protein expression levels of adipose-related genes (PLIN2 and ADIPOR1) ($n = 3$, SD; * $P < .05$; ** $P < .01$; *** $P < .001$). (G) Oil red O staining was used to detect changes in lipid droplets in GLIS2-SG cells caused by GLIS2 knockout or TGF- β 1 induction. (H, I) qRT-PCR and Western blot were used to determine the mRNA and protein expression levels of PPAR- γ targeted genes (FABP4, CD36, and SCD1) in GLIS2-SG cells induced by doxycycline ($n = 3$, SD; * $P < .05$; ** $P < .01$; *** $P < .001$). (J) A dual luciferase assay ($n = 3$) was used to detect the interaction between GLIS2 and the PPAR- γ promoter ($n = 3$). (K) A chromatin immunoprecipitation (IP) assay revealed an interaction between PPAR- γ and the promoters of target genes (FABP4, CD36, and SCD1).

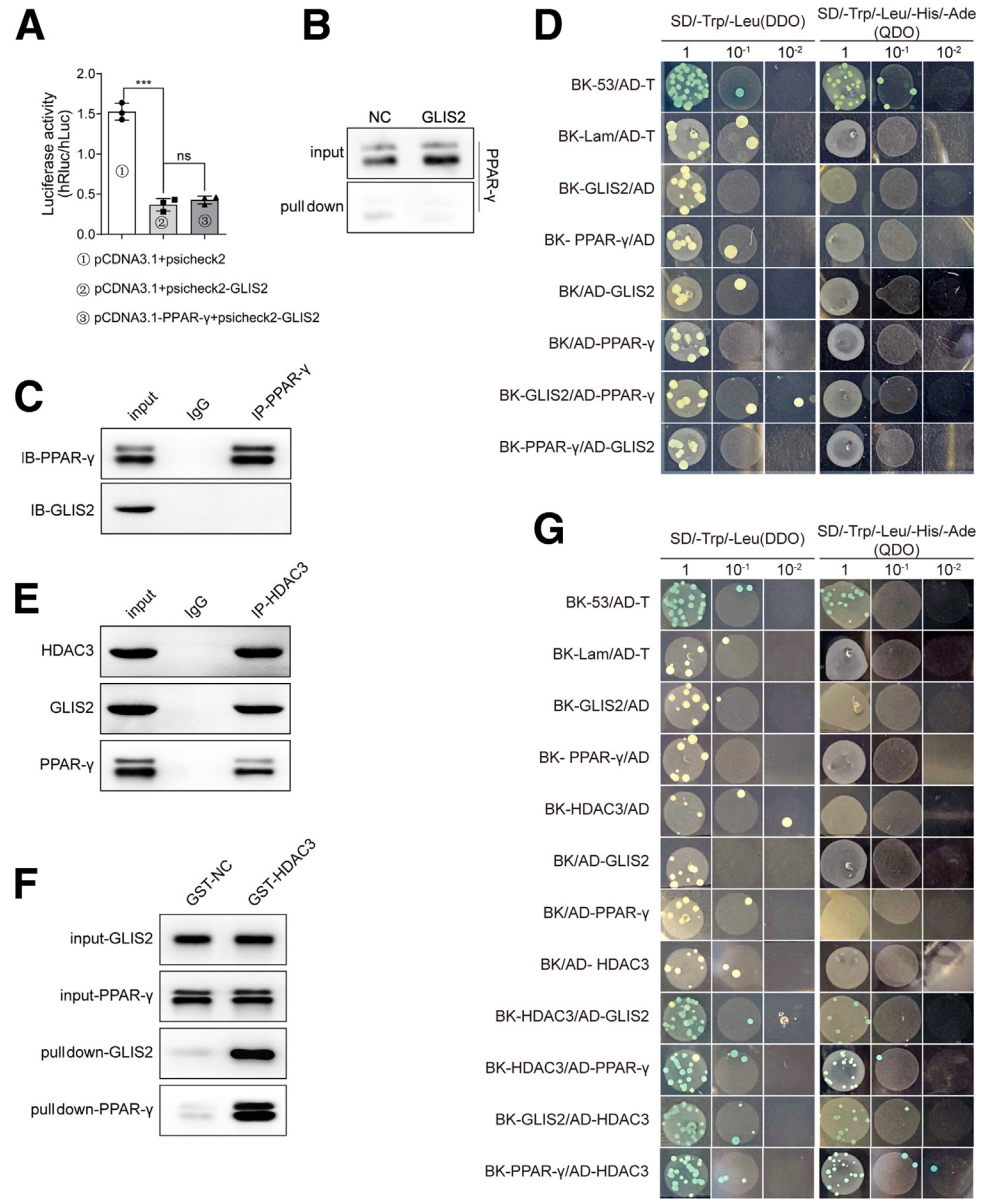


Figure 4. HDAC3 acts as an intermediary for GLIS2 to impress PPAR- γ . (A) Dual luciferase assay ($n = 3$) was used to detect the interaction between the PPAR- γ and GLIS2 promoters ($n = 3$). (B) The GST pull-down assay was used to detect the interaction between GLIS2 and PPAR- γ . (C) A co-IP assay was used to detect the interaction between GLIS2 and PPAR- γ . (D) A yeast two-hybrid assay was used to detect the interaction between GLIS2 and PPAR- γ . (E) A co-IP assay was used to detect the interaction between HDAC3 and PPAR- γ and GLIS2. (F) The GST pull-down assay revealed an interaction between HDAC3 and PPAR- γ and GLIS2. (G) Yeast two-hybrid assay detects the interaction between GLIS2 and PPAR- γ and GLIS2.

cells, the expression levels of PPAR- γ target genes (FABP4, CD36, and SCD1) increased significantly (Figure 7A–C). Meanwhile, GLIS2-SG cells returned to a resting state with slower proliferation rates, lower mobility, and increased lipid droplet storage (Figure 7D–H), similar to the HDAC3 knockout in GLIS2-SG cells.

Furthermore, no significant change in HDAC3 was observed in GLIS2-SG cells (Figure 8A and B), and the acetylation level of PPAR- γ , as well as the status of HSCs, were not changed significantly in GLIS2-SG cells with or without HDAC3 overexpression, but overexpression of GLIS2 or pioglitazone could (Figure 8C–J), indicating that there is a sequential relationship of GLIS2, HDAC3, and

PPAR- γ in regulating stellate cell state. GLIS2 is the most upstream, followed by HDAC3, and the PPAR- γ pathway is the final effector. These findings further suggest that HSCs activation caused by GLIS2 deletion can be reversed by PPAR- γ -acetylation agonists or by reduced expression of the deacetylation enzyme HDAC3.

Overexpression of GLIS2 Ensures the Acetylation Level of PPAR- γ and Alleviates Liver Fibrosis in Mice

The degree of PPAR- γ acetylation in HSCs was reduced in CCL4-induced fibrosis mice, as was the binding abundance in target gene promoter regions (CD36) (Figure 9A and B). We overexpressed GLIS2 in HSCs to treat liver fibrosis.

Table 1. List of Interacting Proteins Predicted by HitPredict

Proteins Bound to GLIS2	Proteins Bound to PPAR- γ
CTBP1	RXRA
Q9JM08 (HDAC3)	NCOA2
	SIR1
	PRGC1
	PIAS2
	FBX9
	PRD16
	MEN1
	F6M2J9
	SP1
	MED14
	HDAC1
	NOCT
	ABL1
	VIME
	DESM
	NEDD4
	CAV1
	TGIF1
	IRF6
	TF65
	SIAH2
	Q2M4I6
	TGF1
	UBP7
	FOXP3
	SMUF1
	WWTR1
	Q9JM08 (HDAC3)

CCL4-induced mice models were treated with a tail vein injection of an adeno-associated virus (AAV), which specifically targets HSCs, to increase GLIS2 expression in vivo (Figure 9C–E). The results showed that the acetylation degree of PPAR- γ increased with AAV treatment, as did the binding abundance of PPAR- γ in the promoter regions of its downstream target genes was found (Figure 9F and G). Meanwhile, the expression of fibrosis-related indicators (α -SMA, Col1 α 1, and TIMP1) was significantly reduced (Figure 9H–I), as were the ALT, AST, and total bilirubin levels in serum samples (Figure 9J). In the AAV-GLIS2 mice, the morphology of liver tissue and histological staining (H&E, Masson, and Sirius red) revealed significant pathological changes and decreased accumulation of collagen fibers (Figure 9K), indicating that fibrosis is significantly alleviated. Overexpression of GLIS2 can thus increase the acetylation level of PPAR- γ and alleviate hepatic fibrosis in CCL4-induced mice hepatic fibrosis.

Discussion

HSCs play critical roles in the development of hepatic fibrosis. The findings of basic and clinical studies indicate that influencing the fate of HSCs can help to prevent and even reverse hepatic fibrosis. As a result, research into the plasticity of HSCs may provide a novel approach to treating chronic liver disease.²⁷ HSCs are a major type of myofibroblast.¹⁴ Transdifferentiation of myofibroblasts from an adipogenic to a myoblast phenotype is an important event

in HSC activation.^{7,28,29} qHSCs store lipid droplets and express neural and adipogenic markers (GFAP, PPAR- γ , PLIN2, ADIPOR1) under normal conditions, but in response to injury, they rapidly upregulate fibrogenic genes (Col1 α 1, α -SMA, TIMP1) and become activated HSCs or myofibroblasts to produce the fibrous scar.²⁸ However, it is unclear what the switch molecules are that determine whether HSCs are activated or resting. In this study, we discovered that deleting GLIS2 in HSCs activates them, and the mechanism is related to the inhibition of the PPAR- γ pathway.

The role of GLIS2 in renal fibrosis is well established, but the role of GLIS2 in hepatic fibrosis is debatable. This study's findings are qualitatively inconsistent with GLIS2 function in mice with hepatic fibrosis caused by a high alcohol diet.³⁰ We discovered that GLIS2-deficient HSCs lost their silent phenotype and became activated, implying that GLIS2 is required to keep HSCs silent. This is consistent with previous findings that GLIS2 deletion causes renal fibrosis in mice.^{9,11} Furthermore, the hedgehog signaling pathway is thought to be involved in HSCs differentiation. It was discovered that it was activated in mouse, rat, and human aHSCs.³¹ Some studies have found that GLIS2 can negatively regulate the hedgehog signal,³² implying that GLIS2 may also inhibit aHSCs, which is consistent with the findings of this study.

PPAR- γ has been identified as the primary regulatory signal in MTD.^{7,14} PPAR- γ was inhibited in aHSCs.^{14,15} When activated, the movement of PPAR- γ from the cytoplasm to the nucleus is reduced, which results in less binding to PPRE elements in the promoter region of downstream target genes, inhibiting transcription. And the acetylation level of PPAR- γ influences this process. In the silent state, the PPAR- γ pathway in HSCs was activated, promoting the lipid storage function of HSCs. The mechanisms, however, are poorly understood. During the mechanism study, we gradually ruled out the possibility of GLIS2 regulating PPAR- γ transcription, PPAR- γ regulating GLIS2 transcription, and GLIS2 and PPAR- γ forming transcription coactivators to regulate MTD. Furthermore, we discovered that HDAC3-mediated deacetylation of PPAR- γ was the link between GLIS2 and PPAR- γ . During HSCs activation caused by GLIS2 deficiency, more HDAC3 bound to PPAR- γ , causing PPAR- γ deacetylation and inhibiting its transcriptional function.

Previous research discovered that the PPRE (which is the binding region of PPAR- γ and the target gene promoter) is made up of an (A/G) GGTCA direct repeat sequence. The ROR α response element, like the PPRE, is composed of a core motif of a 6-base-rich sequence ([A/G] GGTCA). Thus, HDAC3-ROR α was likely to bind to the promoter of the PPAR- γ target gene competitively.^{20,21} Transcription factors binding to the PPRE region of the PPAR- γ target gene promoter were identified using a DNA pulldown assay. We discovered that when GLIS2 is expressed normally, PPRE primarily binds PPAR- γ , whereas when GLIS2 is deficient, PPRE primarily binds HDAC3-ROR α , and in this case, PPAR is inactivated and retained in the cytoplasm rather than

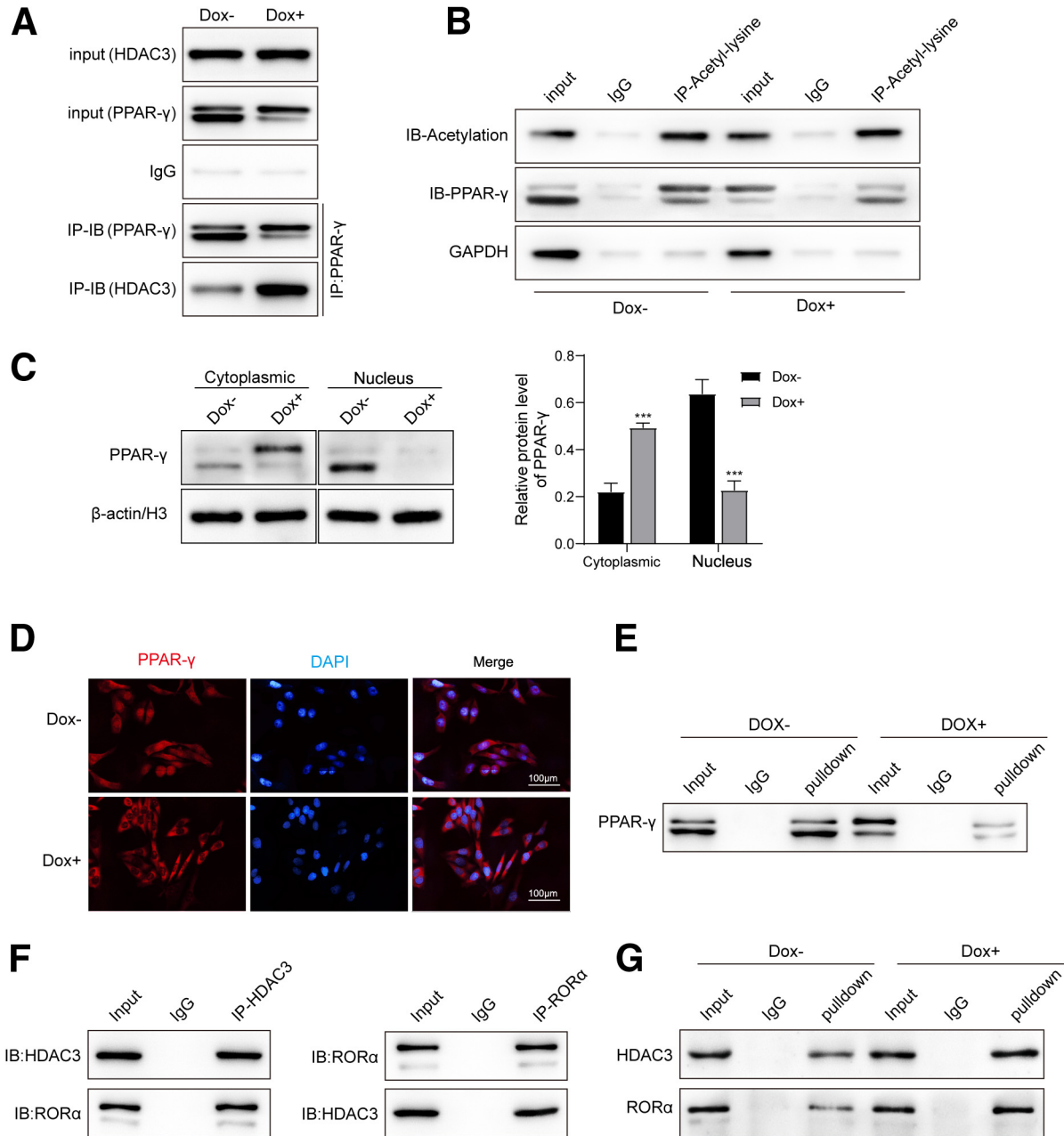


Figure 5. HDAC3 inactivates the PPAR- γ signaling in GLIS2-SG cells. (A) The co-IP assay detected HDAC3 and PPAR- γ binding during HSC activation induced by GLIS2 knockout. (B) PPAR- γ acetylation was detected during the activation of HSCs caused by GLIS2 knockout. (C) Western blot was used to determine the PPAR- γ protein levels in the cytoplasm and nucleus of GLIS2-SG cells induced by doxycycline ($n = 3$, SD; * $P < .05$; ** $P < .01$; *** $P < .001$). H3 was used for cytoplasmic proteins and β -actin was used for extracellular proteins. (D) Immunofluorescence staining was used to detect PPAR- γ protein in GLIS2-SG cells induced by doxycycline. (E) A DNA pull-down assay revealed the presence of PPAR- γ that binds to the CD36 promoter. (F) A co-IP assay was used to detect protein binding between HDAC3 and ROR α in GLIS2-SG cells treated with doxycycline. (G) DNA pull-down assays identified HDAC3-ROR α binders to the CD36 promoter in the GLIS2-SG cells.

entering the nucleus and binding to the PPARE to induce transcriptional activation of target genes.

In conclusion, we propose a novel mechanism for activating HSCs: GLIS2 deficiency causes excessive HDAC3 binding to PPAR- γ and PPAR- γ inactivation, inhibiting

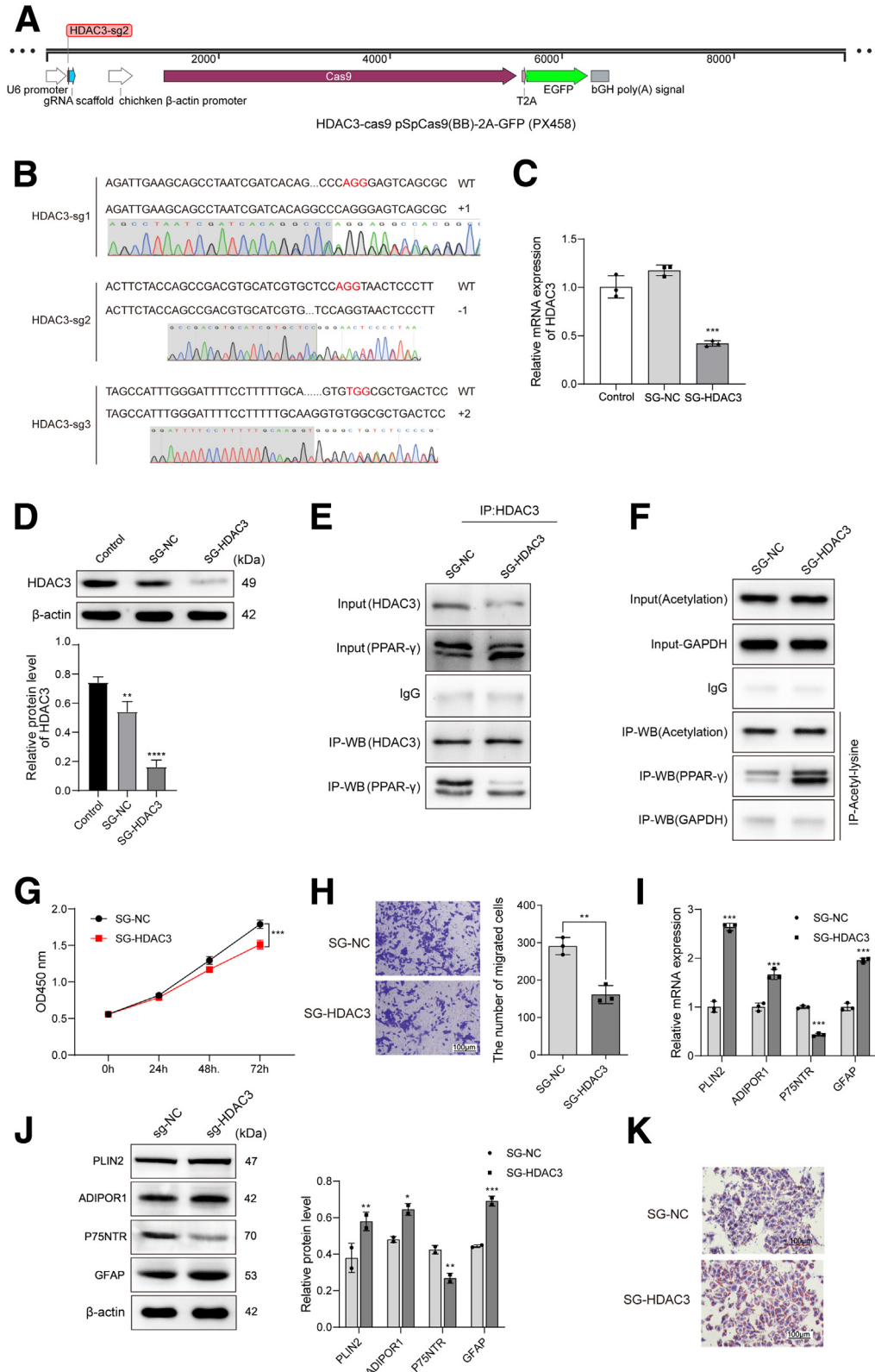
transcriptional activation of target genes. At this point, the adipocyte phenotype transforms into the myoblast phenotype, resulting in the activation of HSCs. These findings add to our understanding of the pathogenesis and prevention of hepatic fibrosis.

Materials and Methods

Experimental Animals and Animal Care

All mice used in this study were C57BL/6 mice 8–10 weeks of age (male, 20 ± 2 g) obtained from Hunan SJA

Laboratory Animals (China). The mice were fed standard rodent food and water and kept in a pathogen-free, climate-controlled environment with a temperature of 25 ± 1°C under 12-hour light/dark cycles. Intraperitoneal injections



of CCl₄ (0.5 μL/g, dissolved in corn oil at a ratio of 1:3) and only corn oil were used to induce hepatic fibrosis. The Institutional Review Board of Third Xiangya Hospital, Central South University, approved the study, which was carried out following the National Institutes of Health Guide for the Care and Use of Laboratory Animals.

Cell Culture and Treatment

BNCC (Beijing, China) provided JS-1 cells (mouse HSC cell line) (BNCC339310). At 37°C and 5% CO₂ in humidified air, JS-1 cells were cultured in Dulbecco's modified Eagle's medium (Gibco, Waltham, MA; 11965118) supplemented with 10% fetal bovine serum (ExCell Bio, Shanghai, China; FSP500), 100 U/mL penicillin, and 100 μg/mL streptomycin (Gibco; 15140163).

Isolation of Primary HSCs

Pronase/collagenase perfusion digestion was used to isolate primary mouse HSCs, followed by density gradient centrifugation, as previously described.³³ In brief, liver tissues were first digested in situ with 0.05% pronase E (Roche, Shanghai, China) and 0.03% collagenase type IV (Sigma-Aldrich, Shanghai, China), and then further digested for 20 minutes at 37°C in a shaking bath with collagenase type IV, pronase E, and DNase I (Roche). Due to a large amount of vitamin A-storing lipid droplets in nonparenchymal cells, HSCs were isolated from them using Nycodenz solution (Sigma-Aldrich) and 4°C. Primary HSCs were cultured in a humidified incubator with 5% CO₂ at 37°C in high-glucose Dulbecco's modified Eagle's medium containing 10% fetal bovine serum and 1% penicillin/streptomycin.

Vector Construction

Cas9 was located behind the TRE3GS promoter, rtTA was initiated by the hPGK promoter, and puromycin was located behind the SV40 promoter in the GLIS2 knockout lentivirus vector based on the CRISPR-Cas9 system regulated by doxycycline. Furthermore, sgRNA targeting GLIS2 was found behind the U6 promoter. Cas9 was expressed to knock out GLIS2 when doxycycline was added. When the doxycycline was removed, Cas9 was stopped, and the designed GLIS2 knockout system no longer worked.

Establishment of GLIS2-SG Cells

Based on the CRISPR/Cas9 system, we constructed a doxycycline-regulated lentivirus vector that targeted the

mouse GLIS2 gene, packaged it into viral particles, and infected JS-1 cells (Figure 3). Three spCas9 (NGG) targets were designed, and the T7E1 assay revealed that the knockout effect of sgRNA-2 (5'-GTCCACCTTCTCAGGGAATT-3') was the best, and it was used in subsequent experiments. Puromycin was used to screen JS-1 after virus infection, and single-cell amplification and cell lines were established. We chose the monoclonal cell line D3 with the highest puroR expression level for subsequent experiments (named GLIS2-SG), after detecting puroR gene continuously started by SV40 promoters. Doxycycline (2 μg/mL) was added during the induction process.

Lentivirus Production and Transduction

For overexpression and knockout experiments, an empty vector served as a negative control. Using LipoFiter (HanBio, Shanghai, China), these constructs were used to generate lentivirus in 293T cells with packaging plasmids using LipoFiter (HB-LLF-1000). Lentiviruses were collected 72 hours after transfection and filtered through a 0.45-μm filter (Millipore, Burlington MA; SLHV033RB). JS-1 cells were then infected with lentivirus for further investigation.

Quantitative Reverse-Transcription Polymerase Chain Reaction and Genomic Polymerase Chain Reaction

TRIzol reagent (Tiangen, Beijing, China; DF424) was used to isolate total RNA from tissues and cells, and the complementary DNA reverse transcription kit was used to create complementary DNA (Takara Bio, San Jose, CA; RR037A). PerfectStart Green qPCR SuperMix (TransGen Biotech, Beijing, China) was used for the quantitative reverse-transcription polymerase chain reaction (qRT-PCR) (AQ601). For normalization, GAPDH was used as an internal control. The 2^{-ΔΔCT} method was used to determine the relative expression of the target gene. Table 2 lists the primers used in this study for qRT-PCR. MicroElute Genomic DNA Kit (Omega Bio-tek, Norcross, GA; D3396) was used to extract genomic DNA according to the manufacturer's instructions. Table 2 contains a list of the PCR primers.

Western Blotting

RIPA was used to extract protein lysates from tissues and cells (Beyotime Biotechnology, Haimen, China; P0013B). BCA protein concentration assay kit (Beyotime Biotechnology; P0012) was used to calculate protein concentration. Sodium dodecyl sulfate polyacrylamide gel electrophoresis

Figure 6. (See previous page). PPAR-γ signal inactivation caused by GLIS2 deficiency can be partially reversed by reducing HDAC3. (A) Mapping of knockout vector containing both sgRNA and Cas9 proteins that target mouse HDAC3. (B) Genomic sequencing revealed that sgRNAs targeting HDAC3 can result in indels. (C, D) qRT-PCR and Western blot were used to confirm the knockout effect of HDAC3 (n = 3, SD; *P < .05; **P < .01; ***P < .001). (E) When HDAC3 was knocked out, the binding of HDAC3 and PPAR-γ was detected using a co-IP assay in GLIS2-SG cells induced by doxycycline. (F) When HDAC3 was knocked out, the PPAR-γ acetylation level was detected in GLIS2-SG cells induced by doxycycline. (G, H) Cell proliferation and migration abilities in GLIS2-SG cells induced by doxycycline were assessed using the CCK-8 assay and the Transwell migration assay when HDAC3 was knocked out. (I, J) When HDAC3 was knocked out, the mRNA and protein expression levels of HSC status-related genes (P75NTR, GFAP) and adipose-related genes (PLIN2 and ADIPOR1) were determined using qRT-PCR and Western blot (n = 3, SD; *P < .05; **P < .01; ***P < .001). (K) Oil red O staining was used to detect changes in lipid droplets in HDAC3 knockout.

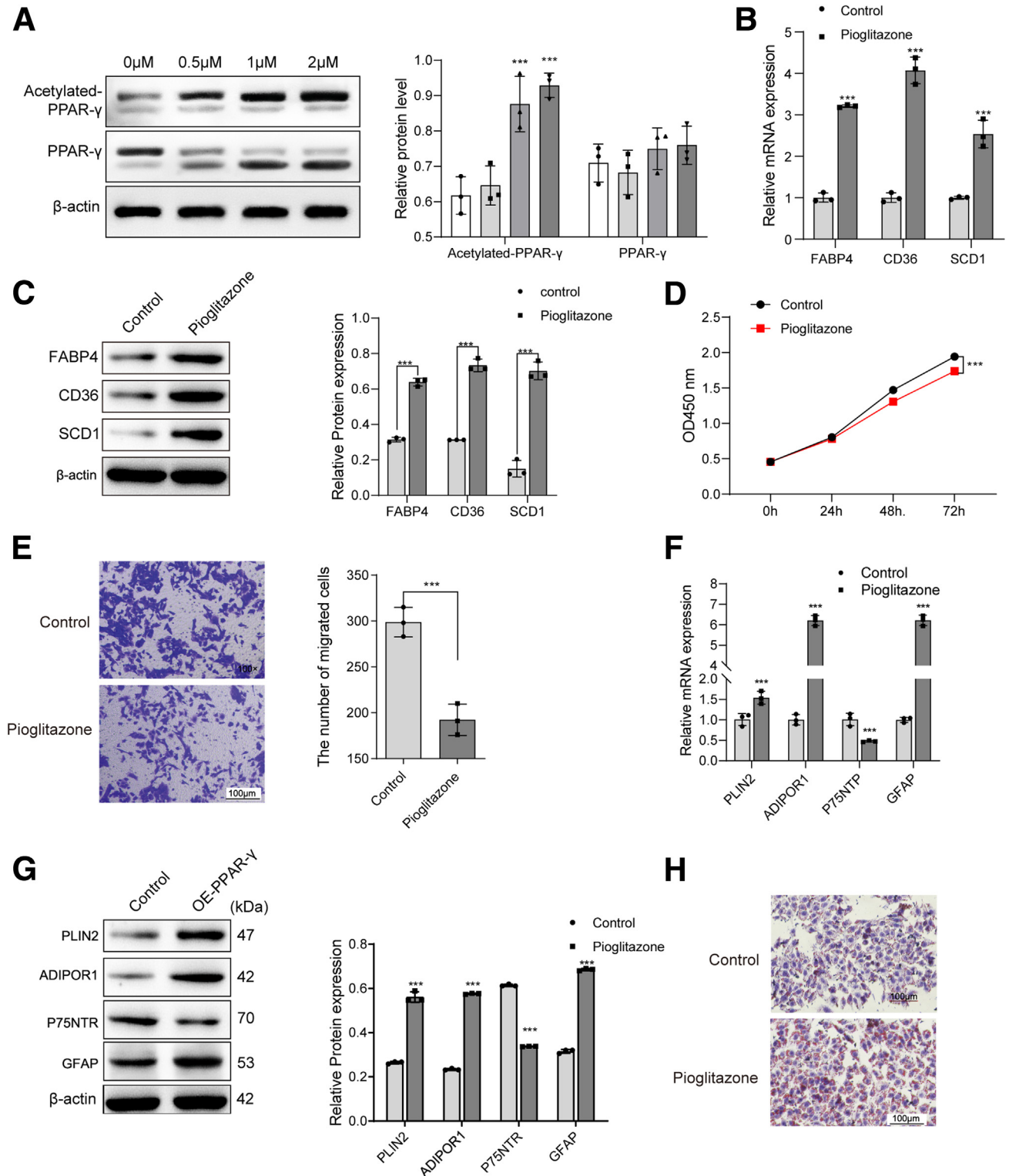


Figure 7. GLIS2 determines HSCs status by influencing PPAR- γ acetylation levels. (A) Screening suitable concentration of pioglitazone and the concentration of 1 μ M were chosen for the subsequent studies after screening. (B, C) qRT-PCR and Western blot were used to determine the mRNA and protein expression levels of PPAR- γ -targeted genes (FABP4, CD36, and SCD1) ($n = 3$, SD; * $P < .05$; ** $P < .01$; *** $P < .001$). (D, E) CCK-8 assay and Transwell migration assay were used to monitor the proliferation and migration abilities of GLIS2-SG cells induced by doxycycline with the pioglitazone addition. (F, G) The levels of mRNA and protein expression of HSC-level status-related genes (P75NTR, GFAP) and adipose-related genes (PLIN2 and ADIPOR1) were determined by qRT-PCR and Western blot with pioglitazone ($n = 3$, SD; * $P < .05$; ** $P < .01$; *** $P < .001$). (H) Oil red O staining with the pioglitazone added detected changes in lipid droplets.

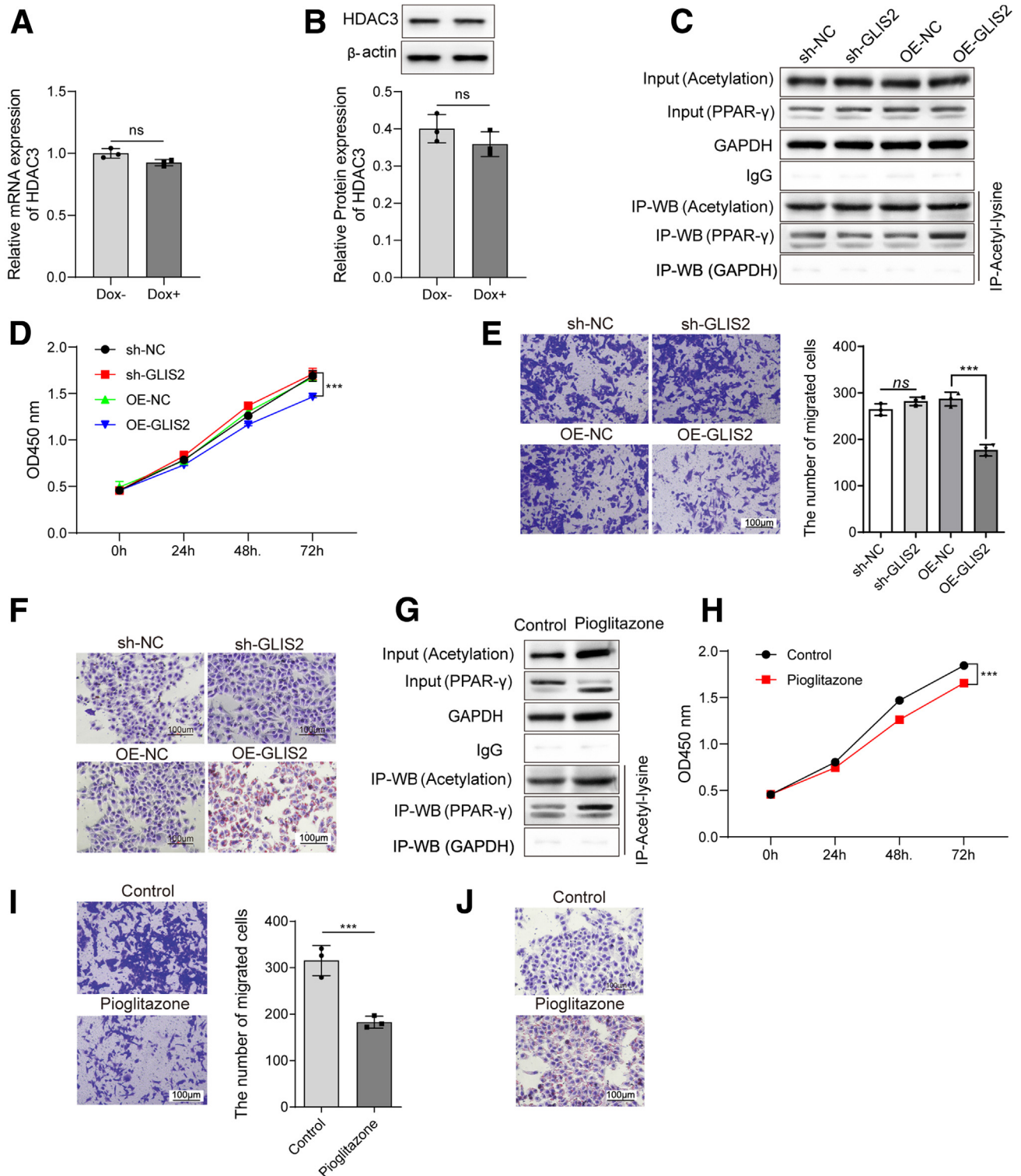
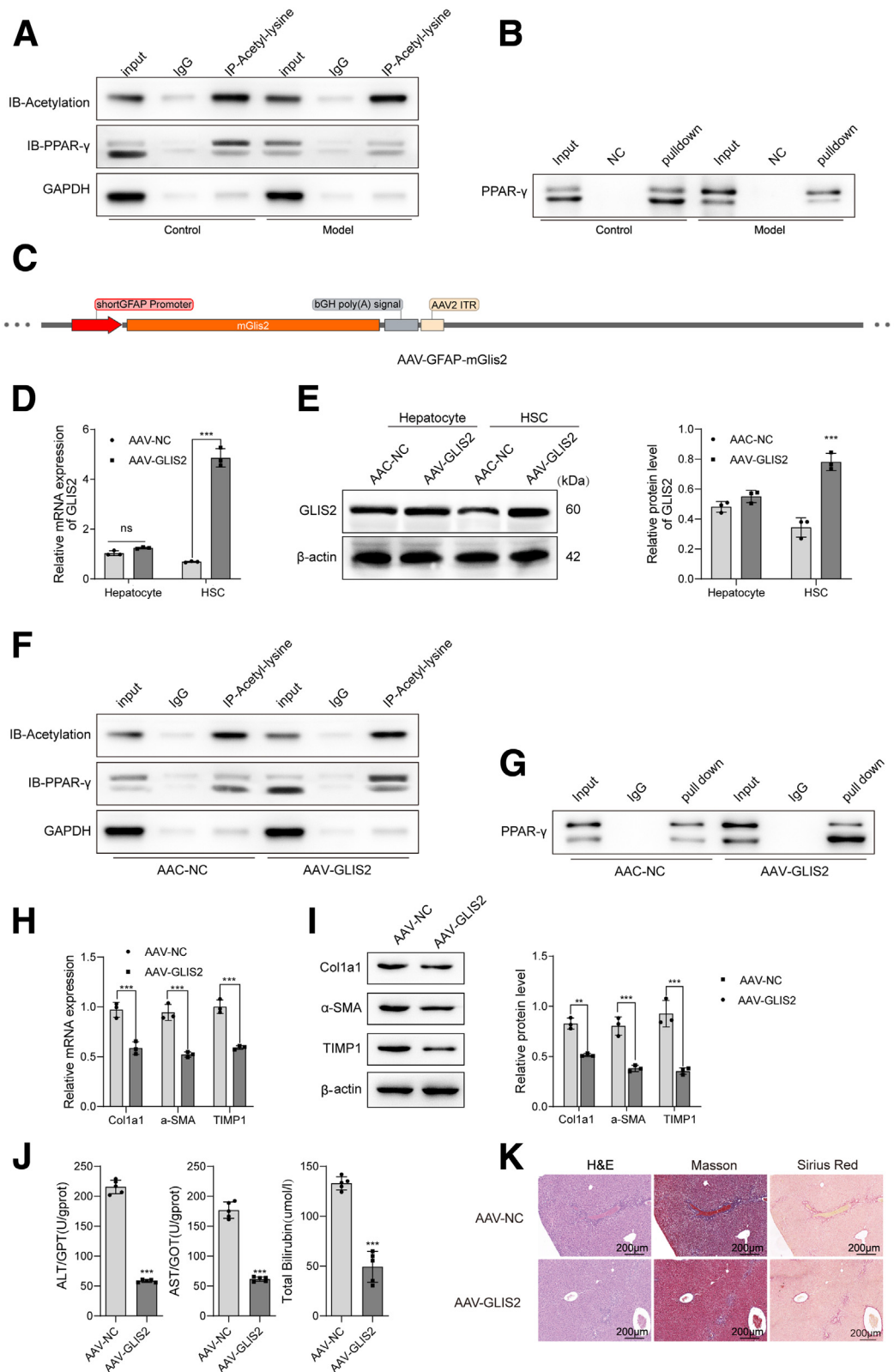


Figure 8. HDAC3 regulates PPAR- γ signaling through competitive binding of GLIS2 or PPAR- γ . (A, B) qRT-PCR and Western blot were used to determine the mRNA and protein expression levels of HDAC3 in GLIS2-SG cells induced by doxycycline ($n = 3$, SD; * $P < .05$; ** $P < .01$; *** $P < .001$). (C) PPAR- γ acetylation was detected in the presence of HDAC3 overexpression and changes in GLIS2 gene expression. (D, E) CCK-8 assay and Transwell migration assay with HDAC3 overexpression and changes in GLIS2 gene expression were used to monitor proliferation and migration abilities. (F) Oil red O staining revealed changes in lipid droplets caused by HDAC3 overexpression and changes in GLIS2 gene expression. (G) PPAR- γ acetylation was detected with HDAC3 overexpression and pioglitazone addition. (H, I) The CCK-8 assay and the Transwell migration assay were used to monitor proliferation and migration abilities in the presence of HDAC3 overexpression and pioglitazone. (J) Oil red O staining was used to detect changes in lipid droplets caused by HDAC3 overexpression and pioglitazone addition.

was used to separate total protein lysates, which were then transferred to polyvinylidene fluoride membranes (Millipore; IPVH00010). The blot was then blocked with 5%

nonfat milk and incubated with the primary antibody overnight at 4°C. After 1 hour of incubation at room temperature with the corresponding horseradish peroxidase-conjugated



secondary antibody, proteins were visualized with BeyoECL Plus (Beyotime Biotechnology; P0018S). ImageJ software (V.1.52, National Institutes of Health, Bethesda, MD) was used to analyze the data, and the figures were cropped. [Table 3](#) lists the primary antibodies used for Western blotting.

Histochemical Staining

Tissues from the liver were fixed in 4% paraformaldehyde (Servicebio, Wuhan, China; G1101-500ML), embedded in paraffin, and sectioned at 5- μ m intervals. Dewaxed, rehydrated paraffin-embedded liver sections were stained with H&E, Masson, and Sirius red.

Immunohistochemistry

Antigen retrieval was performed on paraffin-embedded liver sections after they had been dewaxed and rehydrated. The slides were blocked with 10% normal goat serum before being incubated with the primary antibody overnight at 4°C. Mouse- and rabbit-specific horseradish peroxidase/AEC immunohistochemistry detection kits were used to visualize the signal (Servicebio; G1216/G1215). [Table 3](#) lists the primary antibodies used in immunohistochemistry.

Immunofluorescence

Coverslip-grown cells were fixed in 4% paraformaldehyde, permeabilized in 0.1% Triton X-100, and blocked with 1% bovine serum albumin. The slides were incubated with the primary antibody overnight at 4°C. After that, a CY3 or FITC-conjugated secondary antibody was incubated at room temperature for 1 hour. DAPI was used to mount the slides (Servicebio; G1012). [Table 3](#) lists the primary antibodies used in immunofluorescence.

Serum Chemistries

Total bilirubin, AST, and ALT levels in serum were determined using the manufacturer's instructions (Nanjing Jiancheng Bioengineering Institute, Nanjing, China; C019-1-1/C010-1-1/C009-1-1).

Chromatin Immunoprecipitation PCR and Chromatin Immunoprecipitation qRT-PCR

Cell samples were lysed and ultrasonically broken to yield chromatin fragments ranging in size from 200 to 500 bp. To precipitate the fragments, a PPAR- γ chromatin immunoprecipitation-grade antibody (Santa Cruz, sc-7273)

was used in accordance with the kit manufacturer's instructions (CST, Cat. No.9003). qRT-PCR was used to amplify the promoter fragments of FABP4, CD36, and SCD1 in chromatin immunoprecipitation products, and the results were presented as a percentage of the Input. [Table 2](#) shows the primer sequences for PCR and qRT-PCR.

Co-IP Assay

Phosphate-buffered saline was used to wash the cells before lysing them in lysis buffer (200 mM NaCl, 50 mM Tris-HCl, pH 8.0, and 0.5% NP40). After that, the lysates were mixed with protein A beads (CST, Waltham, MA; 70024) and incubated overnight at 4°C with primary antibodies against anti-PPAR- γ (sc-7273; Santa Cruz Biotechnology, Dallas, TX), anti-HDAC3 (ab32369; Abcam, Boston, MA), anti-ROR α (ab256799; Abcam), or the corresponding normal IgG (acts as negative control). To remove unbound proteins, the beads were washed twice with lysis buffer. To elute the bound proteins, the beads were resuspended in sample buffer, boiled for 3 minutes at 95°C, and immunoblotted.

Luciferase Assay

In 12-well plates, transient transfection was performed in triplicate. JS-1 cells (1×10^5 per well) were cultured for 24 hours before being transfected with plasmid DNA using LipoFiter (HB-LF-1000). To detect transcription factor binding to promoters, we used a dual-luciferase detection system (psiCHECK2). The promoters of PPAR- γ and GLIS2 replaced the SV40 promoter to promote *Renilla luciferase* gene expression, while firefly luciferase served as a control. The luciferase assay was carried out according to the manufacturer's instructions using the luciferase substrate system (Promega, Madison, WI; E1910). At least 3 dates were used to obtain the results.

Yeast Two-Hybrid Assays

Yeast two-hybrid assays were carried out using the Y2H Gold-Gal4 system (Takara Bio; 630498). To prepare the bait and prey constructs, full-length coding sequences of HDAC3, GLIS2, and PPAR- γ in mice were inserted into the pGBKT7 and pGADT7 vectors, respectively, and transformed into yeast strain Y2H Gold. The bait and prey constructs were co-transformed into yeast strain Y2H Gold according to the manufacturer's instructions for the specific yeast 2-hybrid assays (630498). For observation, yeast

Figure 9. (See previous page). Overexpression of GLIS2 ensures the acetylation level of PPAR- γ and alleviates liver fibrosis in mice. (A) PPAR- γ acetylation was detected in HSCs from hepatic fibrosis mice induced by CCL4. (B) DNA pull-down assay identified PPAR- γ that binds to the CD36 promoter in HSCs from mice with hepatic fibrosis induced by CCL4. (C) AAV-GLIS2 virus vector map. The short GFAP promoter controls mGLIS2 expression in the vector. (D, E) GLIS2 overexpression was confirmed in hepatocytes and HSCs using qRT-PCR and Western blot, respectively (n = 5, SD; *P < .05; **P < .01; ***P < .001). (F) PPAR- γ acetylation levels were detected in HSCs from AAV-NC mice and AAC-GLIS2 mice. (G) In AAV-NC mice and AAC-GLIS2 mice, a DNA pull-down assay detected PPAR- γ that binds to the CD36 promoter in HSCs. (H, I) The mRNA and protein expression levels of fibrosis-related genes (α -SMA, Col1 α 1, TIMP1) in liver tissues of AAV-NC mice and AAC-GLIS2 mice were determined by qRT-PCR and Western blot, respectively (n = 3, SD; *P < .05; **P < .01; ***P < .001). (J) Total bilirubin, ALT, and AST serum levels were measured using enzyme-linked immunosorbent assay in AAV-NC and AAC-GLIS2 mice (n = 5, SD; *P < .05; **P < .01; ***P < .001). (K) H&E, Masson, and Sirius red staining were used to examine histological changes in liver tissues in AAV-NC mice and AAC-GLIS2 mice, respectively.

Table 2. Primers for Polymerase Chain Reaction

Primer	Sequence 5'-3'
GAPDH-QPCR-sense	AGCCCAAGATGCCCTTCAGT
GAPDH-QPCR-antisense	CCGTGTTCTACCCCAATG
GLIS2-QPCR-sense	TTCTTCTTGCCCTGGGTTT
GLIS2-QPCR-antisense	AGCTGGTTACTTGGCCC
TGF β R-QPCR-sense	CCGCAACAACGCCATCTATG
TGF β R-QPCR-antisense	TCTCTGCAAGCGCAGCTCTG
α -SMA-QPCR-sense	GTACCACCATGTACCCAGGC
α -SMA-QPCR-antisense	GCTGGAAGGTAGACAGCGAA
Col1 α 1-QPCR-sense	CCCTGGTCCCTCTGGAAATG
Col1 α 1-QPCR-antisense	GGACCTTTGCCCTTCTTT
TIMP1-QPCR-sense	CTCATCAGGGGCCGCTAA
TIMP1-QPCR-antisense	AGGGAAACTGTGCACACC
P75NTR-QPCR-sense	CAACCAGACCGTGTGTGAACCC
P75NTR-QPCR-antisense	CCTGGTAGTAGCCATAGGAGCATC
GFAP-QPCR-sense	GCTCAATGCTGGCTTCAAGG
GFAP-QPCR-antisense	CGAAGCTGGTTCAGTTCAGC
PLIN2-QPCR-sense	GAGCCACAAATTGCGGTTGC
PLIN2-QPCR-antisense	CTGGCAACAATCTCGGACGT
ADIPOR1-QPCR-sense	CGTGTATAAGGTCTGGGAGGGA
ADIPOR1-QPCR-antisense	GTCTGTGGCCATGTAGCAGG
FABP4-QPCR-sense	TAGATGGCGGGGCCCTGGT
FABP4-QPCR-antisense	CATAACACATTCCACCACGAGC
FABP4-CHIP-sense	GGGGTCTTATCCAGTAGGAA
FABP4-CHIP-antisense	GGGAAACAGACTCTGAAACAT
CD36-QPCR-sense	TGCAAGAAGGAAAGCCTGTGT
CD36-QPCR-antisense	CCAGTTATGGGTTCCACATCTAAG
CD36-CHIP-sense	CTGGCTGTCTGGAACCTCAC
CD36-CHIP-antisense	AGGTTACCTGTGGTCACGCT
SCD1-QPCR-sense	GGCGTTCCAGAATGACGTGT
SCD1-QPCR-antisense	CAAGCAGCCAACCCACGTGA
SCD1-CHIP-sense	TTGACCAAGCATCTGGCAAGT
SCD1-CHIP-antisense	CCAAAAAGCCCAACACAATCA
PPAR- γ -QPCR-sense	GCCCTTTGGTGACTTTATGGAGC
PPAR- γ -QPCR-antisense	CTGGGCGGTCTCCACTGAG
HDAC3-QPCR-sense	GACATGTGCCGCTTCCATTCT
HDAC3-QPCR-antisense	AACACTGGGCAGTCATCACC
spCas9-QPCR-sense	CCGCCAGAAGAAGATACACCAG
spCas9-QPCR-antisense	CTCTCCAGTCTGTGGAAGAAGC
PuroR-QPCR/genome-sense	ATCGAGCGGGTCAACCGAG
PuroR-QPCR/genome-antisense	TTCGACGCTCTCCGGCGT
GLIS2-sg1-genome-sense	AGACTATAAATTGGCCTATCCC
GLIS2-sg1-genome-antisense	GGACACGAGTGCCGGTGG
GLIS2-sg2-genome-sense	CCTCAGCCTCTTGGGTGCT
GLIS2-sg2-genome-antisense	GGCACTTGTCAAGGAGCCC
GLIS2-sg3-genome-sense	TGTATGGACACACTCTCAAGGT
GLIS2-sg3-genome-antisense	CAGCGGGTCTTGGCCAGA
HDAC3-genome-sense	TGCCAGGTTGCCACCTTTG
HDAC3-genome-antisense	CCCTGTTGTTACCCTGTCTTA

Table 3. Antibodies Used in the Study

Antibody	Vendor	Catalog No.	Working Dilution
β -actin	Abcam	ab8226	1:2000 (WB); 42 kDa
GLIS2	Invitrogen	PA5-72849	1:1000 (WB); 1:200 (IF); 60 kDa
α -SMA	Proteintech	14395-1-AP	1:1000 (WB); 43 kDa
Col1 α 1	Proteintech	67288-1-Ig	1:5000 (WB); 120–130 kDa
TIMP1	Santa Cruz	sc-21734	1:200 (WB); 31.5 kDa
P75NTR	Proteintech	55014-1-AP	1:500 (WB); 70 kDa
GFAP	Abcam	ab7260	1:5000 (WB); 53 kDa
PLIN2	Proteintech	15294-1-AP	1:1000 (WB); 47 kDa
ADIPOR1	Abcam	ab70362	1 μ g/mL (WB); 42 kDa
FABP4	Proteintech	12802-1-AP	1:5000 (WB); 15 kDa
CD36	Proteintech	18836-1-AP	1:1000 (WB); 88 kDa
SCD1	Santa Cruz	sc-515844	1:500 (WB); 36 kDa
PPAR- γ	Santa Cruz	sc-7273	1:200 (WB); 55 kDa+ 60 kDa
HDAC3	Abcam	ab32369	1:5000 (WB); 49 kDa
ROR α	Abcam	ab256799	1:1000 (WB); 60 kDa+ 65 kDa

IF, immunofluorescence; WB, Western blot.

cells were cultured in various media. The SD/-Trp yeast culture medium is devoid of tryptophan. SD/-Trp-Leu-His yeast culture medium does not contain tryptophan, leucine, or histidine. SD/-Trp-Leu-His-Ade is a culture medium that does not contain tryptophan, leucine, histidine, or adenine.

Acetylation Assay

The lysate was mixed with the cell precipitate, lysed on ice for 30 minutes, and centrifuged, and the supernatant was collected. BCA (Thermo Fisher Scientific, Waltham, MA) was used to determine the protein concentration. Each tube received 5 μ L of A + G beads, which were washed and mixed. Each tube received an antibody (approximately 1 μ g/1 mg protein). In each experiment, the corresponding IgG antibody was used as a control. At the same time, a buffer was added as an input to other tube tubes for direct sample preparation. The mixture was rotated overnight at 4°C, the rotating beads were washed with lysis buffer, and the supernatant was discarded. Samples were prepared in 1 \times sodium dodecyl sulfate buffer, and acetylation was detected using Western blotting.

DNA Pulldown

A DNA pulldown kit was used to perform the assays (BersinBio Company, Guanzhou, China; Bes5004). To isolate the proteins binding to these cis-elements, SCD1 promoter fragments containing a PPAR- γ and HDAC3-ROR α binding site were used. Lac Z functioned as a negative control. PCR was used to generate biotinylated promoter fragments. Tissue/cell nuclear protein extracts

were prepared for DNA pulldown analyses. The biotinylated promoter fragments were immobilized on streptavidin magnetic beads as directed by the manufacturer. To obtain the probe-magnetic bead complex, the mixture was incubated at room temperature for 25 minutes. In the binding buffer, the extracted nucleoproteins were added to the probe-magnetic bead complex. After a 30-minute incubation at 4°C, the mixture was placed on a magnetic rack, and the supernatant was removed. Washing 4 times with wash buffer removed non-specifically bound proteins. Finally, the target protein was eluted with DTT-containing protein elution buffer and identified using Western blotting.

Statistical Analysis

SPSS 21.0 was used for statistical testing (IBM Corp, Armonk, NY). The data were presented as mean \pm SD. Student's *t* test was used to compare the 2 groups. For the comparison of multiple conditions, a 1-way analysis of variance was used. **P* < .05, ***P* < .01, and ****P* < .001 were used to denote statistical significance.

References

- Friedman SL. Hepatic stellate cells: protean, multifunctional, and enigmatic cells of the liver. *Physiol Rev* 2008; 88:125–172.
- Marrone G, Shah VH, Gracia-Sancho J. Sinusoidal communication in liver fibrosis and regeneration. *J Hepatol* 2016;65:608–617.
- Iredale JP. Hepatic Stellate Cell Behavior during resolution of liver injury. *Semin Liver Dis* 2001;21:427–436.
- Khomich O, Ivanov AV, Bartosch B. Metabolic hallmarks of hepatic stellate cells in liver fibrosis. *Cells* 2019;9:24.
- Higashi T, Friedman SL, Hoshida Y. Hepatic stellate cells as key target in liver fibrosis. *Adv Drug Deliv Rev* 2017; 121:27–42.
- Puche JE, Saiman Y, Friedman SL. Hepatic stellate cells and liver fibrosis. *Compr Physiol* 2013;3:1473–1492.
- Tsukamoto H, Zhu NL, Asahina K, et al. Epigenetic cell fate regulation of hepatic stellate cells. *Hepatol Res* 2011;41:675–682.
- Zhang F, Nakanishi G, Kurebayashi S, et al. Characterization of Glis2, a novel gene encoding a Gli-related, Kruppel-like transcription factor with transactivation and repressor functions. Roles in kidney development and neurogenesis. *J Biol Chem* 2002;277:10139–10149.
- Kang HS, ZeRuth G, Lichti-Kaiser K, et al. Gli-similar (Glis) Krüppel-like zinc finger proteins: insights into their physiological functions and critical roles in neonatal diabetes and cystic renal disease. *Histol Histopathol* 2010;25:1481–1496.
- Lichti-Kaiser K, ZeRuth G, Kang HS, et al. Gli-similar proteins: their mechanisms of action, physiological functions, and roles in disease. *Vitam Horm* 2012;88:141–171.
- Kim YS, Kang HS, Herbert R, et al. Kruppel-like zinc finger protein Glis2 is essential for the maintenance of normal renal functions. *Mol Cell Biol* 2008;28:2358–2367.
- She H, Xiong S, Hazra S, et al. Adipogenic transcriptional regulation of hepatic stellate cells. *J Biol Chem* 2005; 280:4959–4967.
- Tsukamoto H. Adipogenic phenotype of hepatic stellate cells. *Alcohol Clin Exp Res* 2005;29:132S–133S.
- Miao CG, Yang YY, He X, et al. Wnt signaling in liver fibrosis: progress, challenges and potential directions. *Biochimie* 2013;95:2326–2335.
- Chhimwal J, Sharma S, Kulurkar P, et al. Crocin attenuates CCl4-induced liver fibrosis via PPAR-gamma mediated modulation of inflammation and fibrogenesis in rats. *Hum Exp Toxicol* 2020;39:1639–1649.
- Moran-Salvador E, Titos E, Rius B, et al. Cell-specific PPARgamma deficiency establishes anti-inflammatory and anti-fibrogenic properties for this nuclear receptor in non-parenchymal liver cells. *J Hepatol* 2013; 59:1045–1053.
- Ding L, Zhou J, Ye L, et al. PPAR-gamma is critical for HDAC3-mediated control of oligodendrocyte progenitor cell proliferation and differentiation after focal demyelination. *Mol Neurobiol* 2020;57:4810–4824.
- Jiang X, Ye X, Guo W, et al. Inhibition of HDAC3 promotes ligand-independent PPARgamma activation by protein acetylation. *J Mol Endocrinol* 2014;53:191–200.
- Borojevic R, Monteiro AN, Vinhas SA, et al. Establishment of a continuous cell line from fibrotic schistosomal granulomas in mice livers. *Vitro Cell Dev Biol* 1985; 21:382–390.
- Kim K, Boo K, Yu YS, et al. RORalpha controls hepatic lipid homeostasis via negative regulation of PPARgamma transcriptional network. *Nat Commun* 2017;8:162.
- Ohoka N, Kato S, Takahashi Y, et al. The orphan nuclear receptor RORalpha restrains adipocyte differentiation through a reduction of C/EBPbeta activity and perilipin gene expression. *Mol Endocrinol* 2009;23:759–771.
- Lin HY, Wang FS, Yang YL, et al. MicroRNA-29a suppresses CD36 to ameliorate high fat diet-induced steatohepatitis and liver fibrosis in mice. *Cells* 2019; 8:1298.
- Patil A, Nakai K, Nakamura H. HitPredict: a database of quality assessed protein-protein interactions in nine species. *Nucleic Acids Res* 2011;39: D744–D749.
- Bhaskara S, Knutson SK, Jiang G, et al. Hdac3 is essential for the maintenance of chromatin structure and genome stability. *Cancer Cell* 2010;18:436–447.
- Lu XF, Cao XY, Zhu YJ, et al. Histone deacetylase 3 promotes liver regeneration and liver cancer cells proliferation through signal transducer and activator of transcription 3 signaling pathway. *Cell Death Dis* 2018; 9:398.
- Bhaskara S, Hiebert SW. Role for histone deacetylase 3 in maintenance of genome stability. *Cell Cycle* 2011; 10:727–728.
- Friedman SL. Evolving challenges in hepatic fibrosis. *Nat Rev Gastroenterol Hepatol* 2010;7:425–436.
- Kisseleva T, Cong M, Paik Y, et al. Myofibroblasts revert to an inactive phenotype during regression of liver fibrosis. *Proc Natl Acad Sci U S A* 2012;109: 9448–9453.

29. Molenaar MR, Vaandrager AB, Helms JB. Some lipid droplets are more equal than others: different metabolic lipid droplet pools in hepatic stellate cells. *Lipid Insights* 2017;10:1178635317747281.
30. Loft A, Alfaro AJ, Schmidt SF, et al. Liver-fibrosis-activated transcriptional networks govern hepatocyte reprogramming and intra-hepatic communication. *Cell Metab* 2021;33:1685–1700.e9.
31. Yang J-J, Tao H, Li J. Hedgehog signaling pathway as key player in liver fibrosis: new insights and perspectives. *Expert Opin Ther Targets* 2014;18:1011–1021.
32. Li B, Rauhauser AA, Dai J, et al. Increased hedgehog signaling in postnatal kidney results in aberrant activation of nephron developmental programs. *Hum Mol Genet* 2011;20:4155–4166.
33. Maschmeyer P, Flach M, Winau F. Seven steps to stellate cells. *J Vis Exp* 2011;51:2710.

Received August 19, 2022. Accepted October 20, 2022.

Correspondence

Address correspondence to: Zhenguo Liu, MD, Department of Infectious Disease, The Third Xiangya Hospital, Central South University, No. 138

Tongzipo Road, Changsha 410013, Hunan Province, People's Republic of China. e-mail: liuzg729@163.com.

Acknowledgments

This study was conducted according to the National Institutes of Health Guide for the Care and Use of Laboratory Animals and was approved by the IRB of Third Xiangya Hospital, Central South University (2020-S076). The informed consent was obtained from study participants. The datasets generated during and/or analyzed during the current study are available from the corresponding author on reasonable request.

CRedit Authorship Contributions

Haoye Zhang (Conceptualization: Lead; Data curation: Equal)
Pengcheng Zhou (Data curation: Equal; Formal analysis: Lead)
Wu Xing (Funding acquisition: Lead)
Limin Chen (Investigation: Lead; Methodology: Lead; Project administration: Lead)
Yangmei Zhou (Supervision: Lead; Validation: Lead)
Hui Yang (Visualization: Lead)
Kangkang Fu (Writing – original draft: Lead)
Zhenguo Liu (Writing – review & editing: Lead)

Conflicts of Interest

The authors disclose no conflicts.

Funding

This study was funded by grants from the National Natural Science Foundation of China (No. 82170639), the Hunan Provincial Natural Science Foundation (No. 2022JJ70068, 2022JJ70070), and the Medical Scientific Research Program of Beijing Medical and Health Foundation (No. YWJKJHKYJJ-BXN006).